Proceedings of the Seventh International Conference on
Artificial Intelligence, Soft Computing, Machine Learning and Optimization,
in Civil, Structural and Environmental Engineering
Edited by: P. Iványi, J. Kruis and B.H.V. Topping
Civil-Comp Conferences, Volume 11, Paper 1.2
Civil-Comp Press, Edinburgh, United Kingdom, 2025
ISSN: 2753-3239, doi: 10.4203/ccc.11.1.2

Conceptualizing an AI-based Effective Stiffness Analysis of Human Trabecular Bone

J. Gebert[1,2], F. Pelzer[1,2] and M. M. Resch[1,2]

[1] High-Performance Computing Center Stuttgart, Germany
[2] Institute for High-Performance Computing, University of Stutttgart, Germany

Abstract

Linear elastic material characterization of human trabecular bone is of interest, for example, to simulate bone-implant systems. The direct mechanics method for computing stiffness tensors of trabeculae based on directly discretized computed tomography scans is proven and available. However, characterizing the effective stiffness based on microfocus CT scans is computationally expensive. We suggest a new, AI-based method for characterizing volume elements used in direct mechanics approaches. The goals are to reduce the required computational effort and cost while keeping a comparable accuracy of the effective stiffness parameters that we can compare to the existing analytical ground truth. Our approach assumes that binary segmented grayscale CT images are 3-dimensional patterns that answer deformations with particular forces and exhibit a specific effective stiffness. The paper describes the assumptions, training data, and software stack for AI training and inference. We conclude with expected results, methodological limits, and an outlook.

Keywords: direct mechanics, finite elements, human bone, high-performance computing, artificial intelligence, effective stiffness, stiffness

1 Introduction

Trabecular bone is a calcified, porous tissue of thin struts and plates as in figure 1, commonly found in, e.g., the scapula, vertebrae, and femur. It is embedded within the bone marrow, forming the spongiosa, and plays a key role in bearing internal and external mechanical loads. Healthy trabecular bone is essential for maintaining mobility and quality of life.

Figure 1: The human femur is a load-bearing bone with an articulate trabecular structure inside [1].

Surgical intervention may be required, e.g., in cases of fractures or chronic conditions like arthrosis, often involving metallic implants [2–4]. These implants vary in shape and function but frequently rely on surrounding trabecular bone for stability. A prominent example is total hip arthroplasty (THA), where a metal stem is implanted into the femur to alleviate pain and restore joint function. However, implants are subject to wear, and their lifespan is limited [5, 6].

Radiological images and anatomical preparations highlight the importance of trabecular bone in preventing implant failure, such as aseptic loosening caused by mechanical rather than inflammatory reasons [7]. Additional factors such as initial implant positioning can affect outcomes, suggesting patient-specific simulations may improve success rates [8]. Governed by Wolff's law and the mechanostat theory, bone remodels continuously to adapt the bone structure in response to mechanical strain [9, 10]. This adaptation process, known as mechanotransduction, operates throughout life [11].

Mechanical models of human bone are of significant research interest because they

allow researchers and engineers to predict and improve the performance of bone-implant systems. Mechanical models allow researchers and engineers to simulate these interactions, account for patient-specific anatomical and material variability, and explore how bones respond to altered loading conditions over time through processes like remodeling. By accurately determining the effective stiffness of bone, mechanical models support the development of longer-lasting, better-integrated implants and inform clinical decisions aimed at reducing revision surgeries and improving patient outcomes.

2 State of Research

The effective stiffness is a boundary condition-driven parameter of, e.g., human trabecular bone with stiffness as the resistance against deformation. Hook's law

$$\sigma_{ij} = C_{ijkl}\epsilon^{kl} \tag{1}$$

contains the stiffness C as a transfer function between the stress σ and the strain ϵ with

$$i, j, k, l \in \{1, 2, 3\} \tag{2}$$

that sum over sets of repeated indices. This notation relies on Einstein's summation convention. Two Lamé constants,

$$\mu = G = \frac{E}{2(1+\nu)} \tag{3}$$

and

$$\lambda = \frac{E\nu}{(1+\nu)(1-2\nu)} \tag{4}$$

connect the Young's modulus E, the poisson ratio ν and the shear modulus G. These well-known engineering parameters give the isotropic stiffness matrix

$$\begin{bmatrix} \sigma_1 \\ \sigma_2 \\ \sigma_3 \\ \sigma_4 \\ \sigma_5 \\ \sigma_6 \end{bmatrix} = \begin{bmatrix} \lambda+2\mu & \lambda & \lambda & 0 & 0 & 0 \\ & \lambda+2\mu & \lambda & 0 & 0 & 0 \\ & & \lambda+2\mu & 0 & 0 & 0 \\ & & & \mu & 0 & 0 \\ & \text{sym.} & & & \mu & 0 \\ & & & & & \mu \end{bmatrix} \begin{bmatrix} \epsilon_1 \\ \epsilon_2 \\ \epsilon_3 \\ \epsilon_4 \\ \epsilon_5 \\ \epsilon_6 \end{bmatrix} \tag{5}$$

to, e.g., describe a monolithic material. Isotropy in mechanics denotes the material's uniformity in all orientations. Human trabecular bone, however, is a heterogeneous, non-repeating structure that exhibits anisotropic behavior. The mathematical description

$$v \begin{bmatrix} \sigma_1 \\ \sigma_2 \\ \sigma_3 \\ \sigma_4 \\ \sigma_5 \\ \sigma_6 \end{bmatrix} = \begin{bmatrix} C_{11} & C_{12} & C_{13} & C_{14} & C_{15} & C_{16} \\ & C_{22} & C_{23} & C_{24} & C_{25} & C_{26} \\ & & C_{33} & C_{34} & C_{35} & C_{36} \\ & & & C_{44} & C_{45} & C_{46} \\ & \text{sym.} & & & C_{55} & C_{56} \\ & & & & & C_{66} \end{bmatrix} \begin{bmatrix} \epsilon_1 \\ \epsilon_2 \\ \epsilon_3 \\ \epsilon_4 \\ \epsilon_5 \\ \epsilon_6 \end{bmatrix} \tag{6}$$

of such a material requires 21 linearly independent parameters. Special cases are described with fewer parameters. For example, orthotropic materials show three perpendicular symmetry planes and only require nine linearly independent parameters.

Various methodologies exist to extract the initially multiaxial linear elastic properties based on fabric tensors that link bone microarchitecture to the fourth-rank stiffness tensor [12]. However, accurate mechanical modeling of the trabecular bone requires the precise but computationally demanding finite element method (FEM) based on direct discretization of micro-CT (mCT) scans as in figure 2 [13].

Figure 2: The microfocus CT scan of a human femoral head with a 3-dimensional equidistant voxel spacing of 15 µm to capture all relevant structural details [14]. Other bone tissues with trabeculae are of interest as well.

High-resolution CT scans, as depicted, are 3-dimensional equidistant voxel grids with image grayscales representing the bone density. The basic characteristic of this exemplary mCT image is given in table 1.

Axes	x	y	z
Dimensions	2940	2940	2141
Resolution (mm)	0.015	0.015	0.015
Number of Voxels	18505947600		

Table 1: Parameters of the exemplary mCT scan `FH01-1`.

For local anisotropy, apparent material properties can be computed for cuboid-shaped volume elements (VEs) under specific boundary conditions. However, representative volume elements (RVEs), which are ideally independent of loading conditions, are theoretically valid only in two scenarios: as unit cells in periodic microstructures or as statistically homogeneous volumes containing an infinite number of infinitesimal elements [15]. Trabecular bone, neither periodic nor infinitely sampled, challenges both assumptions, limiting the theoretical applicability of RVE concepts.

Hill presented a method to compute effective stiffness $\breve{C}$ matrices of VEs. However, these matrices depend on the applied boundary conditions [16, 17]. Computed tomography images are decomposed into many small VEs as shown in figure 3.

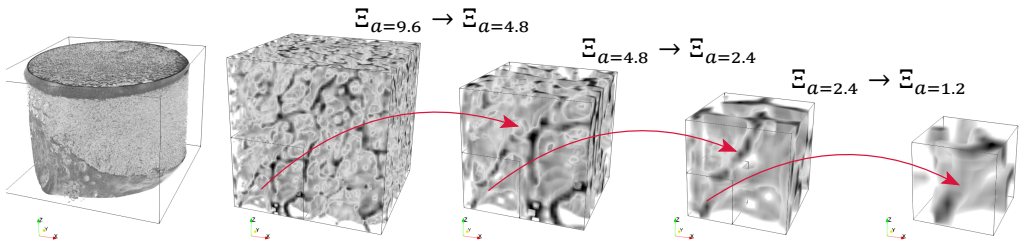

Figure 3: The VE decomposition sizes to extract cuboid subsets of the mCT scan are introduced by Ralf Schneider [18]. Cavities in human trabecular bone govern the smallest sensible VE size, with larger sizes following in increments.

A promising alternative comes from the work of Ralf Schneider, who in 2016 introduced a method to compute effective numerical stiffnesses [18]. These resemble element stiffness matrices and can be used to assign material properties to continuum-level FEs, making them suitable for simulating bone-implant systems. His implementation also computes the effective stiffness with a finite element model and leads to the required 21 linearly independent parameters $\breve{C}_{ij}$. Ralf Schneider's implementation of the directly discretizing voxel-FE conversion with cuboid volume elements is best visible in figure 4, with the outline of the VE shown with grey lines. However, computing linear elastic effective stiffness parameters with large finite element models is compute-intensive, leading to the requirement of high-performance computing (HPC) systems.

The characterization of the patient-specific scan of figure 2 is best described by, e.g., focusing on orthotropic parameters as they already give an impression on the

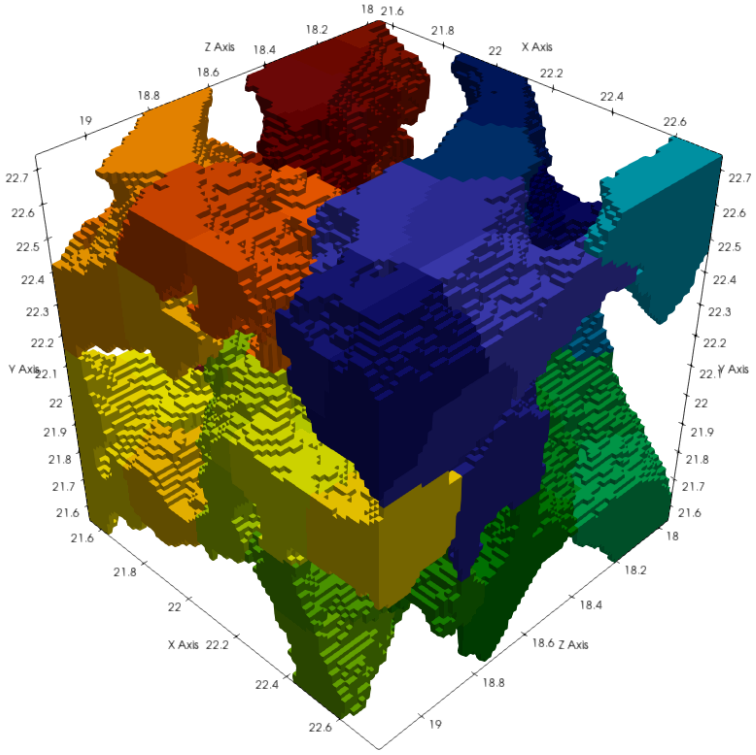

Figure 4: The exemplary cuboid volume element (VE) of edge length $a = 1.2$mm contains a binary segmented bone structure split into sub-meshes for computation on a few too many compute units. The colors represent the assignments to specific processors for computation.

bone's behavior. Since we decompose the CT scan into many volume elements, scatterplots of these VEs material parameters, as in figure 5, can help to derive statistical knowledge about the trabecular bone structure.

3 High-Performance Computing

The software stack called Direct Tensor Computation (DTC), developed by Ralf Schneider and Johannes Gebert, is implemented with Fortran, the Message-Passing Interface (MPI) [19], the Portable, Extensible Toolkit for Scientific Computation (PETSc) [20], and METIS mesh decompositioning [21]. MPI for general communication and PETSc for MPI-based solving of sparse matrix linear algebra allow for massively parallel computations. Computational efforts relating to the VEs Ξ are best quantified as in table 2.

VEs of all sizes are subsets of the mCT image as in figure 2 and table 1; hence, the initial volume of interest is constant. Accordingly, the number of VEs extracted from an mCT can vary. While we can compute up to about 200000 VEs at the minor scale

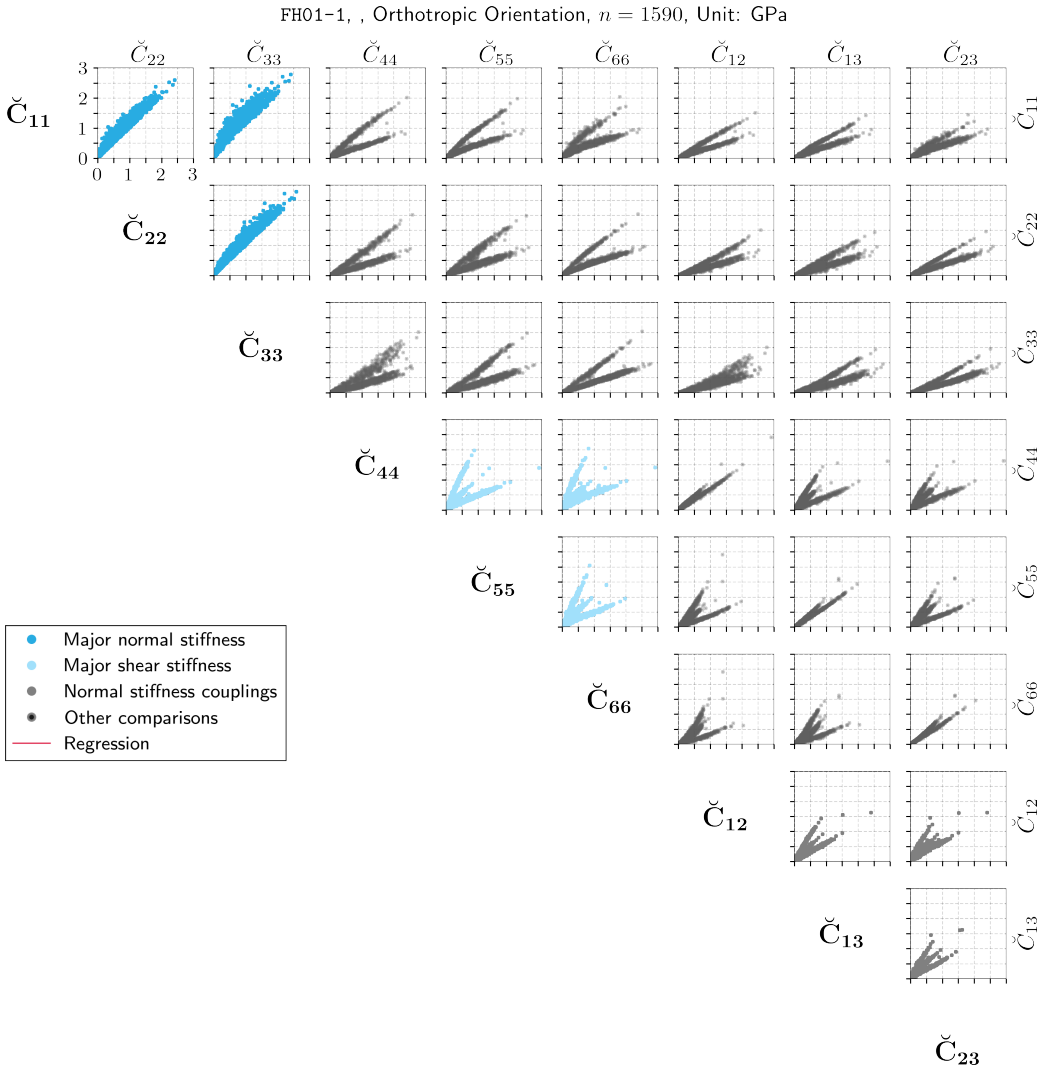

Figure 5: The relationships of the orthotropic material parameters of the CT scan as in figure 2.

with only two processors used per VE, we already need several thousand processors for large VE sizes, but we then deal with a smaller number of VEs to compute.

Not only are thousands of processors running concurrently required, but the memory requirements is also high. We computed the ground truth data on Hawk, a supercomputer of the High-Performance Computing Center Stuttgart (HLRS), Germany. In this case, two gigabytes of memory per core at 128 cores per compute node are available at a total memory bandwidth of 380 $\frac{\text{GB}}{\text{s}}$. The communication across compute nodes relies on an Inifiniband 200 GBit network with the topology of a 9-dimensional hypercube.

From the perspective of a high-performance computing center, high energy usages

Ξ_a (mm)	n_Ξ	n_c
0.6	191825	2 to 16
1.2	25865	2 to 32
2.4	3484	16 to 1024
4.8	455	64 to 2048
7.2	143	2048 to 4096
9.6	40	4096 to 8192

Table 2: VE sizes, numbers of grid-parallel VEs contained in the mCT scan, and the number of processors required.

are an issue from an environmental and a cost perspective with several hundred kWh per simulation, especially for large VE sizes Ξ_a.

From a user's perspective, HPC resources are a significant hurdle to compute, e.g., tensors of human trabecular bone. Since these HPC systems are expensive and their operation is complex, the biomechanical researcher does not have these computers at hand; he instead has to apply to compute with them. In addition, the software must support the hardware environment of the supercomputer, a task that might be straightforward with readily available software. Setting up the computing environment may take a few years if the researcher needs to write software from scratch.

All in all, there is a justification for methods to avoid using HPC resources.

4 Research Question

Previous sections outlined the biomechanical motivation, goal, and implications of using HPC systems required for a direct mechanics approach with high-resolution CTs. Hence, we formulate a straightforward research question: Can we significantly reduce the computational effort without losing the accuracy of the solution? With the previous research by Ralf Schneider, precise data on all VE sizes and their mechanical behavior are available as the ground truth for any comparison with our AI-based approach.

5 AI-based effective Stiffness

Based on our experience using AI in HPC applications, we assume that binary segmented grayscale CT images are 3-dimensional patterns that answer deformations with highly specific forces and, therefore, exhibit a quantifiable effective stiffness. AI systems are renowned for their ability to recognize patterns. However, we must prove that the anisotropic parameters, expressed as floating point numbers, are accurately determined during inferencing.

We expect an answer to the research question by providing readily trained neural networks that can run on common workstations rather than on HPC systems. Suppose we observe a high correlation ($r^2 > 0.9$) between the analytical ground truth and the AI-based anisotropic parameters. In that case, we can reduce the computational effort and lower the boundaries to access this method in clinical, industrial, or research environments.

This paper does not present the final results but suggests a method. Our goal is to describe a path to AI-driven direct mechanics approaches and discuss potential pitfalls.

5.1 Approach

We rely on two major components to solve the research question. First, we use the CT data in their corresponding volume element to provide an input image. Second, we know the ground truth through the analytical analysis as described in previous sections. The input CT images of all VEs are assigned their corresponding effective stiffness with up to 21 linearly independent parameters to describe the linear elastic mechanical anisotropy. We then train the neural network with about two-thirds of the available data. Once the training is completed, we analyze the AI's accuracy by inferencing the test VEs, which consists of the remaining third of the available data. Furthermore, we decided to start training different neural network architectures. In addition, we increase the complexity by starting with

- six out of 21 linearly independent parameters $\breve{C}_{ij}$,
- continue with orthotropy (nine of of 21 parameters), and
- extend the method to the full set of 21 parameters.

We proceed with these listed steps once the neural network architecture is promising and the results are reasonable. Both aspects will be the subject of ongoing discussion.

To predict the effective stiffness tensors from 3-dimensional image data, we begin with convolutional neural networks (CNNs). CNNs have shown great potential in image processing considering their relatively simple architecture [22]. Such networks are especially suitable for classification tasks, which are different from our approach because predicting entries of a 4$^{\text{th}}$ order tensor is well suited for regression. Therefore, we process the output of the convolutional layers using fully connected linear layers. The last layer will not use an activation function in order not to limit the range of values for tensor component entries. Training on the dataset of figure 2 with a voxel spacing Ξ_s of 15 µm and the exemplary cuboid VE's edge length Ξ_a gives

$$n_{vox} = \left\lfloor \frac{\Xi_a}{\Xi_s} \right\rfloor^3 = \left\lfloor \frac{0.6\text{mm}}{0.015\text{mm}} \right\rfloor^3 = 64.000 \tag{7}$$

voxels per VE. All neural networks therefore require a high-dimensional input, no matter the actual VE size.

5.2 Software Stack

We aim to process biomechanical data based on image processing and regression methods. For choosing the software stack, we consider the underlying biomechanical complexity and the rationale of the bitter lesson by Richard Sutton [23]. We, therefore, do not aim for complex initial networks or training techniques; rather, we aim for a large amount of verified and correct training data.

The image data of the volume elements is read from `*.vtk` files and converted to numpy arrays by calling the vtk python libary [24]. We use Pytorch [25] to set up the neural network's architecture. In order to train the network, we map each volume element to its corresponding analytical effective stiffness tensor. The Pandas library [26] is used to read and process `*.csv` resembling files that contain the analytical stiffness tensor for each volume element.

5.3 Training data

Supervised learning benefits from a large amount of training data, while overfitting has to be avoided [27]. As per table 2, the VE size $\Xi_{a=0.6}$ allows for the largest number of samples. Hence, we start with this decomposition. Other VE sizes Ξ_a will follow once the characteristics of the neural network are understood. Large Ξ_a results in comparably few available VEs for training and test inferences. For example, $\Xi_{a=2.4}$ only provides 3484 VEs with a verified mechanical tensor available.

Getting more training data is of significant interest to improve the results of the method. However, the number of CT scans analyzed by analytical direct mechanics computations is scarce as the CT scans and HPC resources are expensive. To overcome these limitations, we multiply the existing data by tilting the input images by 90 degrees per step in all available spatial orientations that are grid parallel to the original coordinate system. Since the VEs are cubes with the same number of equidistant voxels in all three dimensions, the VEs are always fed into the neural network similarly without the neural network recognizing that it reads the same VE several times. It is crucial to correctly represent the tilting of the VEs in their corresponding effective stiffness tensor, which we use as a ground truth for training and inferencing. Additionally, the VEs can rotate 90 degrees around their x, y, and z axes, giving four positions per VE surface. By adjusting the effective stiffness tensors accordingly, up to 24 configurations of the identical, verified ground truth are available, rendering in large quantities of training data. If further research shows that even more training data is required, we may mirror existing VEs. Entirely artificial, analytically verified training data can be computed using synthetic structures. However, mirrored and synthetic VEs require careful consideration of their validity for training an AI that analyzes human trabecular bone.

Microfocus computed tomography images are grayscale data used as a proxy for CT absorption. The absorption of X-rays closely correlates with the tissue's density, which, again, is a proxy for the elasticity and other mechanical parameters of the tis-

sue depicted by the corresponding voxel. As implemented by Ralf Schneider, direct mechanics approaches rely on a binary segmentation [18]. Software converts all voxels above a user-defined threshold to a finite element. For the AI-based approach, we still use binary segmented data. The reason is the resulting pattern, which we expect to simplify the neural network's task. In later stages, non-segmented, original data are of interest.

6 Conclusions

We describe a probable path towards effective stiffness tensors of human trabecular bone based on microfocus computed tomography data, which we infer with an AI. The neural network-based approach for image and shape recognition with result vectors representing mechanical stiffness tensors is considered feasible. We have clarified all the steps required to train a suitable neural network and infer future results.

Near future research will confirm or neglect our method. More refined networks and training data will improve the results. However, we will have to prove if the precision of the results suffices for clinical applications or industrial usage with different materials.

References

[1] S. Dorozhkin, Epple, "M. Biological and Medical Significance of Calcium Phosphates", Angewandte Chemie International Edition, 41, 3130-3146, 2002.

[2] D. Apostu, O. Lucaciu, C. Berce, D. Lucaciu, D. Cosma, "Current methods of preventing aseptic loosening and improving osseointegration of titanium implants in cementless total hip arthroplasty: a review.", The Journal Of International Medical Research, 46, 2104-2119, 2017.

[3] R. Laskin, M. Van Steijn, "Total knee replacement for patients with patellofemoral arthritis", Clinical Orthopaedics And Related Research, 89-95, 1999.

[4] M. Merola, S. Affatato, "Materials for Hip Prostheses: A Review of Wear and Loading Considerations", Materials, 12, 495, 2019.

[5] C. Chu, Short-term Analysis vs Long-term Data on Total Hip Replacement Survivorship. JAMA Surgery, 150, 989, 2015.

[6] J. Gallo, V. Havranek, J. Zapletalova, "Risk factors for accelerated polyethylene wear and osteolysis in ABG I total hip arthroplasty", Int Orthop, 34, 19-26, 2009.

[7] J. Pajarinen, E. Jämsen, Y. Konttinen, S. Goodman, "Innate Immune Reactions in Septic and Aseptic Osteolysis Around Hip Implants", Journal Of Long-term Effects Of Medical Implants, 24, 283-296, 2014.

[8] A. Perillo-Marcone, L. Ryd, K. Johnsson, M. Taylor, "A combined RSA and FE study of the implanted proximal tibia: correlation of the post-operative me-

chanical environment with implant migration", Journal Of Biomechanics, 37, 1205-1213, 2004.
[9] J. Wolff, "Das Gesetz der Transformation der Knochen", Pro Business, 2010.
[10] R. Huiskes, R. Ruimerman, G. Van Lenthe, J. Janssen, "Effects of mechanical forces on maintenance and adaptation of form in trabecular bone", Nature, 405, 704-706, 2000.
[11] H. Frost, "Bone's mechanostat: a 2003 update", The Anatomical Record. Part A, Discoveries In Molecular, Cellular, And Evolutionary Biology, 275, 1081-1101, 2003.
[12] P. Zysset, A. Curnier, "An alternative model for anisotropic elasticity based on fabric tensors", Mechanics Of Materials, 21, 243-250, 1995.
[13] S. Cowin, "The relationship between the elasticity tensor and the fabric tensor", Mechanics Of Materials, 4, 137-147, 1985.
[14] M. Ruf, H. Steeb, J. Gebert, R. Schneider, P. Helwig, "Sample 1 of human femoral heads: micro-XRCT data sets", DaRUS, 2021.
[15] B. Van Rietbergen, A. Odgaard, J. Kabel, R. Huiskes, "Direct mechanics assessment of elastic symmetries and properties of trabecular bone architecture", J. Biomech., 29, 1653-1657, 1996.
[16] R. Hill, "Elastic properties of reinforced solids: Some theoretical principles", Journal Of The Mechanics And Physics Of Solids, 11, 357-372, 1963.
[17] D. Pahr, P. Zysset, "Influence of boundary conditions on computed apparent elastic properties of cancellous bone", Biomechanics And Modeling In Mechanobiology, 2008.
[18] R. Schneider, "Analyse kontinuumsmechanischer, anisotroper Materialparameter mikrostrukturierter Volumina mit Hilfe direkter mechanischer Simulation", University of Stuttgart, 2016.
[19] Message Passing Interface Forum, "MPI: A Message-Passing Interface Standard Version 4.0", 2021.
[20] S. Balay, S. Abhyankar, M. Adams, S. Benson, J. Brown, P. Brune, K. Buschelman, E. Constantinescu, L. Dalcin, A. Dener, V. Eijkhout, J. Faibussowitsch, W. Gropp, V. Hapla, T. Isaac, P. Jolivet, D. Karpeev, D. Kaushik, M. Knepley, F. Kong, S. Kruger, D. May, L. McInnes, R. Mills, L. Mitchell, T. Munson, J. Roman, K. Rupp, P. Sanan, J. Sarich, B. Smith, S. Zampini, H. Zhang,Zhang, H. Zhang, J., "PETSc/TAO Users Manual", Argonne National Laboratory, 2023.
[21] G. Karypis, V. Kumar, "METIS: A software package for partitioning unstructured graphs, partitioning meshes, and computing fill-reducing orderings of sparse matrices", 1997.
[22] K. O'Shea, R. Nash, "An Introduction to Convolutional Neural Networks", 2015.
[23] R. Sutton, "The Bitter Lesson", 2019.
[24] W. Schroeder, K. Martin, B. Lorensen, "The Visualization Toolkit (4th ed.)", Kitware, 2006.
[25] A. Paszke, S. Gross, F. Massa, A. Lerer, J. Bradbury, G. Chanan, T. Killeen, Z. Lin, N. Gimelshein, L. Antiga, A. Desmaison, A. Köpf, E. Yang, Z. DeVito, M. Raison, A. Tejani, S. Chilamkurthy, B. Steiner, L. Fang, J. Bai, S. Chintala, "Py-

Torch: An Imperative Style, High-Performance Deep Learning Library", 2019.
[26] T. Team, "pandas-dev/pandas: Pandas", Zenodo, 2020.
[27] P. Domingos, "A few useful things to know about machine learning", Commun. ACM, 55, 78-87, 2012.